Chemical Engineering Journal 103 (2004) 89–97

Chemical Engineering Journal

www.elsevier.com/locate/cej

Kinetics of propylene hydrogenation on nanostructured palladium clusters

Lúcia Brandão[a], Detlev Fritsch[b], Luis M. Madeira[a], Adélio M. Mendes[a,*]

[a] *LEPAE – Departamento de Engenharia Química, Faculdade de Engenharia, Universidade do Porto, R. Dr. Roberto Frias, 4200-465 Porto, Portugal*
[b] *GKSS Forschungszentrum Geesthacht, P.O. Box 1160, D-21494 Geesthacht, Germany*

Received 21 May 2004; received in revised form 28 July 2004; accepted 28 July 2004

Abstract

Surfactant-stabilised palladium nanoclusters with an average diameter of about 7.3 nm (determined by XRD) are used as catalysts in propylene hydrogenation. Experiments performed in an isothermal batch reactor (T = 308 K), with total pressures in the range 0.25–9.0 bar and with initial hydrogen molar ratios varying between 0.05 and 0.40, provide a further insight on the reaction kinetics. It is shown that a Langmuir–Hinshelwood rate equation well represents the reaction data, which mechanism involves competitive adsorption of the reagents, with dissociation of hydrogen on the catalyst surface, and where surface reaction is the limiting step. Nonlinear optimization of the initial rate data provided the kinetic parameters of the rate law (k = 5.569 mol g_{Pd}^{-1} s^{-1}; $K_{H_2} = 3.799 \times 10^{-2}$ bar^{-1} and $K_{C_3H_6} = 0.996$ bar^{-1}), which is validated by integration of the mass balance in the batch reactor.

Keywords: Palladium; Nanoclusters; Propylene; Hydrogenation; Kinetics; Reaction engineering

1. Introduction

Nanoclusters have a significant potential as new types of more active and selective catalysts. Because of their size, generally less than 10 nm, they often display unique catalytic properties. Possible reasons for that are: (i) a large percentage of nanoclusters metal atoms lies on the surface, and thus the surface to volume ratio drastically increases; and (ii) surface atoms do not necessarily order themselves in the same way that those in the bulk do [1].

Nanoclusters are agglomerates of a few to a few thousand atoms. Some clusters of noble metals, e.g. Pd, Ag or Au, were already synthesized by reduction of the metal ions in solution. The metal atoms form a cluster and an organic ligand (e.g. surfactant, polymer) binds to the cluster surface. The ligand shell stabilises the cluster and prevents its agglomeration, because as soon as these nanoclusters come into contact with each other, they agglomerate to lower their surface energy [2,3].

Most studies concerning the catalytic activity of polymer-stabilised nanoclusters have been conducted in solution. For instance, nanoclusters impregnated in Al_2O_3 pellets showed to be three times more active in cyclooctene hydrogenation than a comparable, commercially available, industrial catalyst (5% Pd on Al_2O_3) [4]. A comparatively small number of studies has been undertaken to examine the catalytic activity of metals in polymer-based nanocomposite materials in the presence of gaseous reagents, and some exceptions are their use in hydrogenation reactions [5,6].

Hydrogenation of olefins is an active subject of research and has been one of the most thoroughly studied chemical processes [7,8]. In what concerns its mechanism, it has been generally accepted that hydrogenation of olefins over transition metal catalysts proceeds via an associative mechanism through σ-alkyl intermediates, known as Houriuti–Polanyi mechanism [9]. However, metals also tend to form allylic species by abstracting hydrogen from the olefin (dissociative mechanism) [10].

* Corresponding author. Tel.: +351 22 508 1695; fax: +351 22 508 1449.
E-mail address: mendes@fe.up.pt (A.M. Mendes).

1385-8947/$ – see front matter © 2004 Elsevier B.V. All rights reserved.
doi:10.1016/j.cej.2004.07.008

Nomenclature

C_{i_s}	concentration of the limiting reactant *i* at surface conditions (mol m^{-3})
De	effective diffusivity coefficient (m^2 s^{-1})
K_i	adsorption equilibrium constant for species *i* (bar^{-1})
k	rate constant for the overall hydrogenation reaction (mol g_{Pd}^{-1} s)
k'	rate constant for the surface reaction (mol g_{Pd}^{2} s^{-1} sites^{-3})
m	number of experimental data
M	vacant active site
MSC	model selection criterion
$[M]_T$	total concentration of active sites (sites g^{-1})
p	number of fitting parameters
P	total absolute pressure (bar)
P_i, P_j	partial pressure of species *i*, *j* (bar)
n_i	number of moles of species *i* (mol)
n	number of reactive moles (mol)
R	gas constant (m^3 bar mol^{-1} K^{-1})
R_p	particle radius (m)
r_i	reaction rate for species *i* (mol g_{Pd}^{-1} s^{-1})
r_{obs}	observed reaction rate (mol g_{Pd}^{-1} s^{-1})
T	temperature (K)
t	time (s)
V	reactor volume (m^3)
w	mass of catalyst (g)
X	advancement of the reaction (dimensionless)
X_{max}	maximum advancement of the reaction (dimensionless)
y_i, y_j	molar fraction of species *i*, *j* (dimensionless)

Greek letters

α	fitting parameter of model 2
β	fitting parameter of model 2
ξ	extent or degree of advancement of the reaction (mol)
ν_i	stoichiometric coefficient for species *i*
ρ_c	density of the catalyst pellet (g cm^{-3})
Φ_s	experimental parameter, analogous to Weisz Prater modulus (dimensionless)

Subscripts

I	inert species (argon)
i	species present in the reactor, i.e. H_2, C_3H_6, C_3H_8 or inert
j	reactant species present in the reactor, i.e. H_2 or C_3H_6
o	initial conditions

In the case of ethylene hydrogenation, several mechanisms have been proposed in the literature [8,11]. For instance, Zaera and Öfner [8] suggested a simple Langmuir model that considers competitive adsorption between hydrogen and ethylene. Hydrogen adsorbs dissociatively and the rate-limiting step is the hydrogenation of the ethyl intermediate with adsorbed surface hydrogen [8]. Propylene hydrogenation has not been studied so extensively as ethylene hydrogenation, and most of the works have been focused on the use of a platinum catalyst [12–15]. For both reactions, the kinetics and mechanisms are far from being settled, particularly over a Pd catalyst, which is widely used in industrial practice in hydrogenation reactions.

As most of the hydrogenations take place at temperatures below 200 °C, or even at room temperature, a polymeric catalytic membrane reactor (PCMR) can advantageously be used. But to have access to the parameters governing the separation and the chemical reaction kinetics in a continuous PCMR, independent experiments should ideally be performed. Thus, in the present study, the kinetic parameters of propylene hydrogenation are determined using palladium nanoclusters, which show no mass transport resistances. This data will be important for subsequent modelling of the process in a PCMR and, besides, give more insight concerning kinetics over metal nanoclusters, which is a recent and innovative topic in catalysis.

2. Experimental

2.1. Catalysts preparation

The nanostructured palladium clusters were stabilised using the surfactant tetraoctadecylammonium bromide, *n*-$(C_{18}H_{37})_4N^+Br^-$ [2], whose preparation procedure is reported elsewhere [16,17]. For immobilising these nanoparticles in a porous support (polyester textile), 17.0–20.0 mg of the powder-catalyst, containing 15.71% Pd (w/w), was dispersed in THF (p.a. Merck) at a concentration of 0.20% (w_{Pd}/w). Ultrasound was used for a better dispersion. One drop of the suspension was then released in each square of a previously defined grid (0.6 cm × 0.6 cm) over the porous textile support (5.4 cm × 4.2 cm).

2.2. Catalysts characterization

The average diameter of the surfactant-stabilised palladium clusters was measured using X-ray diffraction (XRD) in a Ditral Siemens D5000 apparatus, employing Cu Kα radiation. The powder was pressed into a squared support (1 cm × 1 cm) and the average diameter was calculated using the Bragg Brentano geometry.

The active surface area of the clusters was obtained from the CO adsorption isotherm, which was determined at 308 K using the gravimetric method in the pressure range of 5–100 mbar.

The palladium-containing samples were also analysed by scanning electron microscopy (SEM) using a Jeol JSM-6301F apparatus, in conjunction with energy dispersive X-ray spectroscopy (EDS) with a Noran-Voyager equipment, both operating at 20 keV. The specimens were firstly processed by means of a Jeol JFC 1100 ion sputtering device for fine gold coating of the surface, to provide stability and conductivity under the electron beams.

2.3. Catalytic experiments

The hydrogenation kinetics of propylene to propane was studied in a jacketed batch cylindrical reactor ($V = 0.55 \times 10^{-3}$ m^3; i.d. = 8.2 cm; h = 10.5 cm), to which a pressure sensor (Druck-PMP 4000 Series—2 or 10 bar, absolute) and a thermocouple were attached. All the gases admitted to the stainless-steel reactor were supplied by Praxair (propylene 99.5%, hydrogen 99.999% and argon 99.999%) and were previously mixed in a jacketed tank, which was connected to the reactor through an on–off valve. Both pressure history and temperature were monitored along the runs, being recorded in a computer at a frequency of 0.1 s^{-1}. The porous support containing the Pd nanoclusters catalyst was attached to a magnetic bar (with a cross shape and stirring at 600 rpm), and this assembly was inserted into the batch reactor.

Palladium oxide formed on the catalyst surface due to air exposition was removed by admitting 1.0 bar of hydrogen into the reactor, leaving for 20 h, and then evacuating with a rotary vacuum pump (maximum vacuum of 10^{-3} mbar). This procedure was repeated twice, as recommended by Sachs et al. [18], and was followed by dilution in argon and a final evacuation. Using the experimental procedure described, reproducible runs were achieved in most of the experimental conditions. However, at high pressures ($P > 4$ bar), some deactivation of the catalyst was noticed. In that case, a new support was prepared with fresh catalyst.

It is known that under catalytic conditions with partial pressures above the deci-Pascal range, and around room temperature, the hydrogenation of small olefins occurs in the presence of carbonaceous deposits (alkylidynes), seen as spectator species that just block the metal surface sites [7,19,20]. In our experimental conditions, it is expected that the surface might be saturated with propylidyne deposits, but such surface coverage should not change under typical experimental conditions. Otherwise, activity decay would be noticed in subsequent experiments.

In the catalytic runs, hydrogen molar ratios in the range 0.05–0.40 were used, at an initial total pressure of 1.0 bar. A set of experiments where the initial total pressure was varied between 0.25 and 9.0 bar (absolute) was also performed, at equal composition ($(y_{H_2})_o = 0.10$ and $(y_{C_3H_6})_o = 0.35$). Both the fraction of inert (argon) and the temperature were the same in all runs: 0.55 and 308 K, respectively. Experiments were repeated at least three times, randomly, and were reproducible within ±5%. Blank runs were also performed, using the support and the magnetic bar, and showed neither catalytic activity nor adsorption of reagents.

The parameters of the rate law were obtained by solving a nonlinear least squares problem using a commercial statistics software (JMP^{TM}). For integration of the mass balances, the time-dependent equations were solved using LSODA [21].

In order to evaluate if internal resistances to mass transfer were significant within the nanostructured palladium clusters, due to the presence of the surfactant, well-known intraparticle transport criteria were used [22]. First, to assess the effective diffusivity coefficients, some experiments were carried out in which 3.0 g of n-$(C_{18}H_{37})_4N^+Br^-$ powder (supplied by Sigma–Aldrich; assay: >98%) was used and the uptake curves determined, through the volumetric method. The experiments have shown that, for all gases considered, the amounts adsorbed are negligible and equilibrium is reached almost instantaneously (ca. 1 s). Comparison of these curves with a mass balance for spherical particles gave us an estimate for the effective diffusivity coefficient ($De \sim 2.6 \times 10^{-7}$ m^2 s^{-1}), assuming 1% deviation from a flat concentration gradient. The following parameter was then evaluated for the maximum particle size found (ca. 20 μm, see below): $\Phi_s = ((r_{obs}\rho_c R_p^2)/(DeC_{i_s}))$, which expresses the ratio of chemical reaction rate to diffusive flux (r_{obs} is the observed reaction rate; $\rho_c \sim 1.8$ g cm^{-3} is the density of the catalyst pellet, obtained by He pycnometry; R_p is the radius of the particle; and C_{i_s} is the concentration of the limiting reactant at surface conditions). Both the Weisz [23] and Hudgins [24] criteria were applied, after fitting different power-law kinetics to our data. These criteria were always verified (Φ_s sufficiently small), thus supporting that internal mass transfer resistances are negligible, and so the hydrogenation reaction proceeds in kinetic regime.

The possible existence of external resistances to mass transfer was also evaluated. For that, different rotation speeds were employed during the experiments. Changing the rotation speed from 0 up to 600 rpm did not change the reaction rate, thus evidencing that external mass transfer effects were absent.

3. Results

3.1. Catalysts characterization

Data from XRD analyses indicated that the average diameter of the surfactant-stabilised palladium clusters is 7.3 ± 2.0 nm, corresponding to a surface area of about 68 m^2 g_{Pd}^{-1} (assuming spherical Pd nanoparticles). The active surface area of this sample was obtained from CO chemisorption. The amount of carbon monoxide adsorbed on the Pd surface was calculated from the plateau of the isotherm, which evidenced that the monolayer capacity of Pd is 4.53×10^{-5} mol g^{-1} of sample. Assuming that 0.5 CO/Pd_s is the average maximum coverage over the exposed palladium [25], the active surface area in the nanostructured palladium clusters is 27 m^2 g_{Pd}^{-1}

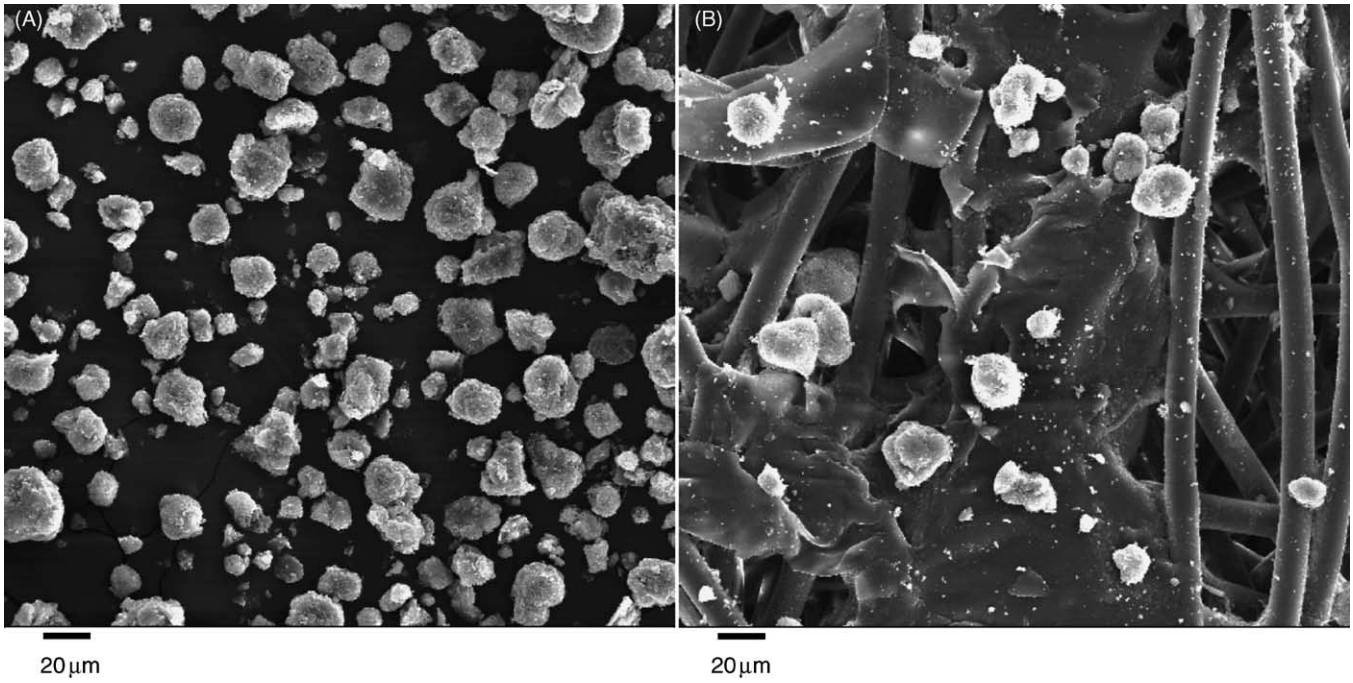

Fig. 1. SEM micrographs of the original nanostructured Pd powder-catalyst (A) and after immobilisation in the textile support (B), both at a magnification of 350×.

(metallic dispersion of 6.1%). This active surface area is significantly different from the surface area computed considering the diameter obtained by XRD. This might indicate that not all sites are active or the chemisorption stoichiometry is not the assumed one. Anyway, these methods should not be directly compared as they use different approaches to obtain the average sizes of the particles populations [26].

Both the size and the active surface of palladium were determined in a sample before dispersion in THF, i.e. in the unsupported catalyst. Because the mass of Pd used in the textile support is very small, those parameters were not evaluated in the supported sample.

SEM/EDS techniques were used to evaluate if the procedure adopted to immobilise the nanostructured palladium clusters in the textile support affects the structure or size of the catalyst aggregates and, eventually, removed the surfactant shell, thus leading to the possible Pd nanoclusters agglomeration. SEM analyses were performed for the powder-catalyst before (Fig. 1A) and after immobilisation (Fig. 1B). One can see that the size of the aggregated clusters on the support is retained, with the biggest particles being in both cases about 20 μm in diameter. Besides, EDS analysis showed the existence of Br (due to the surfactant used) in the immobilised samples and also proved the existence of Pd inside the particles. Therefore, the technique used to immobilise the catalyst does not liberate the Pd clusters from the shell. Palladium nanoclusters were found to be arranged inside surfactant particles as seeds in a pomegranate.

3.2. Catalytic experiments

As above-mentioned, experiments performed in the batch reactor provided total pressure versus time curves, what allowed us to compute the reaction rates. For that, the following concepts were used: (i) extent or degree of advancement of a reaction, ξ, defined as [27,28]

$$\xi = \frac{n_i - n_{i_o}}{\nu_i} \tag{1}$$

where n_i and n_{i_o} are the mole number of species i present in the reactor at instant t and at the initial instant, respectively, and ν_i is the stoichiometric coefficient for species i (so that it is positive for products and negative for reagents); and (ii) normalised advancement:

$$X = \frac{\xi}{n_o} \tag{2}$$

where n_o is the total number of reactive moles at the beginning of the run. Using these concepts, and assuming ideal gas behaviour for the gaseous mixture, it can be easily deduced that

$$X = \frac{1 - P/P_o}{1 - y_{\mathrm{I}_o}} \tag{3}$$

The total fraction of inert gas, y_{I_o}, was kept constant in all runs (0.55). Thus, from experimentally recorded pressure data, advancement results are easily calculated with Eq. (3). Reaction rates, per weight of catalyst, were computed using Eq. (4),

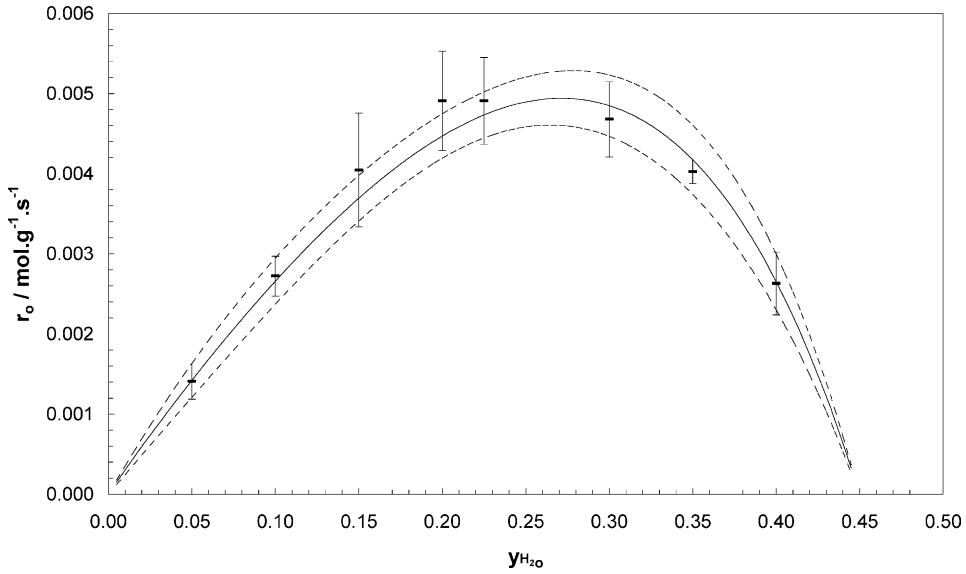

Fig. 2. Effect of the initial hydrogen molar fraction in the initial rates of propylene hydrogenation (P_o = 1.0 bar; y_{I_o} = 0.55; T = 308 K) (—: experimental values). The bar errors for the mean values were obtained for a 95% confidence level (t distribution), using at least three experimental results. The solid line corresponds to the model fitting and dashed lines are the confidence curves (for a 95% confidence level).

which was deduced from a mass balance to the batch reactor.

$$r = \frac{P_o V(1 - y_{I_o})}{wRT} \frac{dX}{dt} \quad (4)$$

In this equation, w denotes the mass of catalyst used and V the reactor volume.

The methodology adopted to deduce the rate law for propylene hydrogenation over the palladium nanoclusters, under isothermal conditions, was the method of initial rates, firstly proposed by Yang and Hougen [29]. The analysis proposed by Yang and Hougen, i.e. the graphical evaluation of the effect of some initial operating conditions (namely total pressure or reaction mixture composition) over the initial rates, still shows to be a useful tool in kinetic modelling, and can save much time and effort.

First, the initial rates of propylene hydrogenation under different initial compositions of the reaction mixture (propylene to hydrogen ratio) were determined at 1.0 bar. Obviously, initial rates were obtained from the slopes of X versus t curves for initial instant (see Eq. (4)). The plot shown in Fig. 2 points

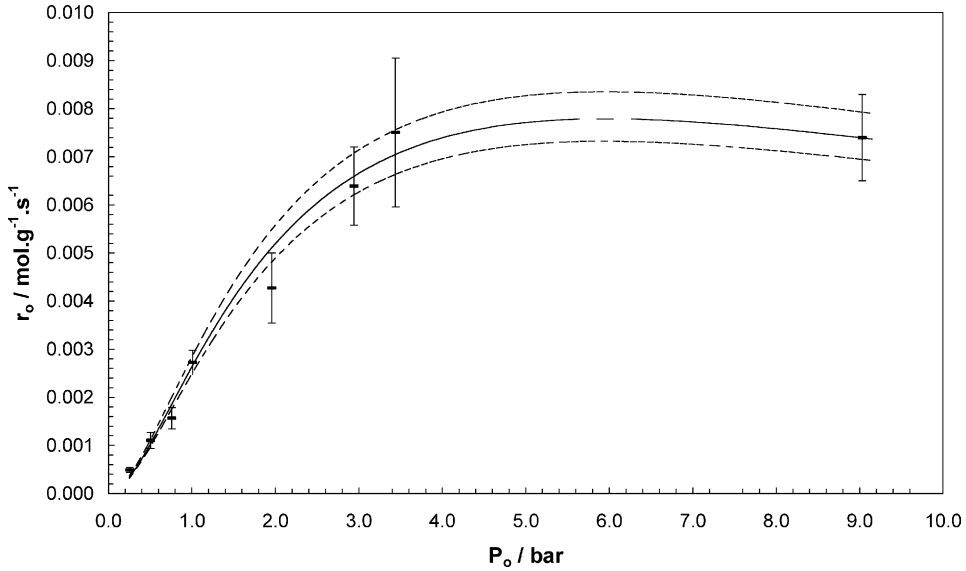

Fig. 3. Effect of the initial total pressure in the initial rates of propylene hydrogenation ($(y_{H_2})_o : (y_{C_3H_6})_o = 0.10 : 0.35$; T = 308 K) (—: experimental values). The bar errors for the mean values were obtained for a 95% confidence level (t distribution), using at least three experimental results. The solid line corresponds to the model fitting and dashed lines are the confidence curves (for a 95% confidence level).

to a mechanism where surface reaction is the limiting step [29], which is in agreement with previous works [30]. More recently, Zaera and Öfner [8] found, using a molecular beam technique at low temperatures and ultra high vacuum, that a competition exists between ethylene and hydrogen for surface sites. They addressed that an increase of hydrogen adsorbed at the surface of the catalyst increases the initial hydrogenation rate, and that a further increase in the surface coverage by hydrogen leads to a slower amount of adsorbed ethylene [8]. Fig. 2 also shows that at high hydrogen concentrations, the initial rate decreases, possibly due to the mentioned competitive adsorption. Such competition leads to a decrease in the number of sites available for propylene adsorption, and consequently in the reaction rate.

The effect of total pressure in the initial hydrogenation rate is illustrated in Fig. 3. Once again, the graphical methodology proposed by Yang and Hougen [29] indicates, from the shape of the curve, and taking also into account data from Fig. 2, that both hydrogen and propylene adsorb on the catalyst, with surface reaction as the limiting step. However, it is not possible to definitely state if dissociation occurs or not because the expected maximum that appears for dissociative adsorption is not very clear in Fig. 3, although it seems to exist. Nevertheless, the dissociative adsorption of hydrogen on the catalyst surface was considered in the proposed mechanism because it provides the best fit to the experimental data, as mentioned below. Besides, this is a well-known phenomenon which occurs on metallic surfaces and widely reported in the literature [31,32].

4. Discussion

From the experiments described, one can determine the kinetic parameters of propylene hydrogenation over palladium nanosized clusters. According to the findings mentioned above, the reaction mechanism can be described by the following steps:

$$H_2(g) + 2M \rightleftarrows 2H{-}M \quad (5)$$

$$C_3H_6(g) + M \rightleftarrows C_3H_6{=}M \quad (6)$$

$$C_3H_6{=}M + 2H{-}M \xrightarrow{k'} C_3H_8(g) + 3M \quad (7)$$

Eq. (5) takes into account the dissociative adsorption of hydrogen on palladium active sites (M), while Eq. (6) describes the adsorption/desorption equilibrium for propylene. Finally, Eq. (7) describes the hydrogenation of adsorbed propylene to propane. Assuming that the surface reaction is the limiting step, and using the Langmuir–Hinshelwood (LH) formulation [28,29], i.e. assuming that the total concentration of active sites $[M]_T$ is constant with a steady-state approximation for Eqs. (5) and (6), it can be easily deduced that the overall rate of propane formation is given by

$$r_{C_3H_8} = \frac{kK_{H_2}K_{C_3H_6}P_{H_2}P_{C_3H_6}}{(1+\sqrt{K_{H_2}P_{H_2}}+K_{C_3H_6}P_{C_3H_6})^3} \quad (8)$$

where $k = k'[M]_T^3$ (k' is the rate constant for the surface reaction (7)) and K_i and P_i represent the adsorption equilibrium constant and partial pressure for species i, respectively. This rate equation evidences the competitive adsorption of both reagents with dissociation of hydrogen on the catalyst surface, which follows the Houriuti–Polanyi mechanism [9]. However, these authors suggest the involvement of two active sites for adsorption of the olefin.

Öfner and Zaera [8] reported a competitive adsorption for Pt (1 1 1) sites between di-σ-bonded ethylene molecules and hydrogen. This di-σ-bonded is a strongly bonded state of adsorption of ethylene that at saturation evolutes to a weakly bonded state (π-bonded ethylene), which is the state that is hydrogenated [8]. More recently, Öfner and Zaera [33] also reported an adsorption mechanism at high coverages of ethylene which involves this π-bonded adsorption. After an initial interaction with the few metal atoms left exposed by an imperfect monolayer, a collective rearrangement of the neighbouring molecules occurs, leading to a new compressed layer (the above-mentioned weakly bonded state). This supports the involvement of one single site, not two, for adsorption of the olefin, similarly to the mechanism herein proposed.

Table 1
Kinetic parameters of propylene hydrogenation over palladium nanoclusters (T = 308 K)

Parameter	Value
k (mol g_{Pd}^{-1} s^{-1})	5.569
K_{H_2} (bar^{-1})	3.799×10^{-2}
$K_{C_3H_6}$ (bar^{-1})	0.996

The parameters of Eq. (8) were determined by a nonlinear regression analysis, by fitting the rate law to the data shown in Figs. 2 and 3. The parameters obtained according to our model are shown in Table 1. Limits for a 95% confidence level are also plotted in Figs. 2 and 3, showing a good model adhesion to the experimental values. However, parameters k and K_{H_2} are linked and the criterion used, minimization of the square residuals, did not allow to obtain high precision values for them.

A great advantage of using nanosized materials is that the surface to volume ratio increases drastically and the surface atoms include an increasing fraction of the total particulate volume with high defect structures. However, it was not possible to compare the catalytic activity of the palladium nanoclusters with other works, as the majority of propylene hydrogenations are reported over platinum catalysts. In the very few studies found where this hydrogenation was carried out over palladium, the experimental conditions employed were out of the range herein adopted.

Based on the same experimental data, the methodology adopted does not exclude other rate equations or reaction

Table 2
Initial reaction rate equations employed to fit the propylene hydrogenation data and corresponding model selection criterion values

Model no.	$(r_{C_3H_8})_o$	Reference	MSC
1	$\frac{kK_{H_2}K_{C_3H_6}(P_{H_2})_o(P_{C_3H_6})_o}{(1+\sqrt{K_{H_2}(P_{H_2})_o}+K_{C_3H_6}(P_{C_3H_6})_o)^3}$		7.25
2	$\frac{\alpha K_{H_2}K_{C_3H_6}(P_{H_2})_o(P_{C_3H_6})_o}{(1+K_{H_2}(P_{H_2})_o+K_{C_3H_6}(P_{C_3H_6})_o)^2}+\frac{\beta K_{H_2}K_{C_3H_6}(P_{H_2})_o(P_{C_3H_6})_o}{(1+K_{H_2}(P_{H_2})_o)(1+K_{H_2}(P_{H_2})_o+K_{C_3H_6}(P_{C_3H_6})_o)}$	[13]	7.16
3	$\frac{kK_{H_2}K_{C_3H_6}(P_{H_2})_o(P_{C_3H_6})_o}{(1+K_{H_2}(P_{H_2})_o+K_{C_3H_6}(P_{C_3H_6})_o)^2}$		6.48
4	$kK_{H_2}K_{C_3H_6}(P_{H_2})_o(P_{C_3H_6})_o\left(\frac{-(1+\sqrt{K_{H_2}(P_{H_2})_o})+\sqrt{(1+\sqrt{K_{H_2}(P_{H_2})_o})^2+4K_{C_3H_6}(P_{C_3H_6})_o[M]_T}}{2K_{C_3H_6}(P_{C_3H_6})_o}\right)^4$		5.83
5	$\frac{kK_{C_3H_6}(P_{H_2})_o(P_{C_3H_6})_o}{(1+K_{C_3H_6}(P_{C_3H_6})_o)^2}$	[35]	5.76
6	$\frac{k\sqrt{K_{H_2}(P_{H_2})_o}K_{C_3H_6}(P_{C_3H_6})_o}{(1+\sqrt{K_{H_2}(P_{H_2})_o}+K_{C_3H_6}(P_{C_3H_6})_o)^2}$	[8]	5.47
7	$\frac{kK_{H_2}(P_{H_2})_o(P_{C_3H_6})_o}{(1+\sqrt{K_{H_2}(P_{H_2})_o})^2}$		2.37

mechanisms. With this in mind, we decided to test different promising reaction mechanisms. The following model selection criterion was adopted [34]:

$$\mathrm{MSC} = \ln\left[\frac{\sum_{i=1}^{m}(r_{o_{\mathrm{obs},i}}-\overline{r_{o_{\mathrm{obs}}}})^2}{\sum_{i=1}^{m}(r_{o_{\mathrm{obs},i}}-r_{o_{\mathrm{cal},i}})^2}\right]-\frac{2p}{m} \quad (9)$$

where m is the number of experimental points, p is the number of fitting parameters and $\overline{r_{o_{\mathrm{obs}}}}$ is the mean of the experimental results. The MSC adopted gives higher values both for models that fit better and for models with less number of parameters, and therefore allows comparison of different models.

Table 2 shows the models considered, ranked by the MSC value. Model 2 was proposed by Rogers et al. and takes into account competitive and noncompetitive adsorption of the reagents at the catalyst surface [13]. Model 3 is a LH equation for a mechanism with surface reaction between adsorbed species controlling, but without hydrogen dissocia-

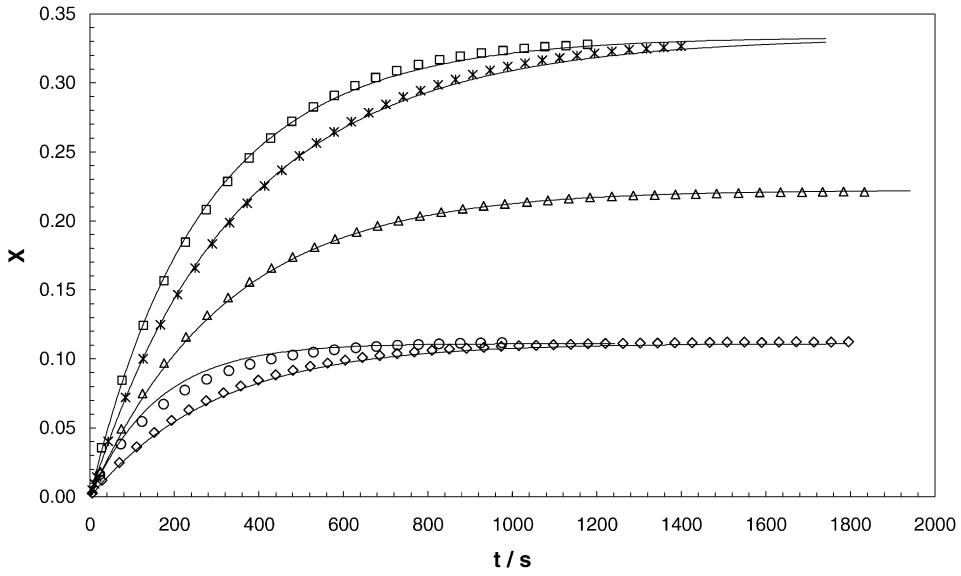

Fig. 4. Advancement of the reaction as a function of time for different initial compositions of the reaction mixture: $(y_{H_2})_o = 0.05$ (◇), $(y_{H_2})_o = 0.10$ (△), $(y_{H_2})_o = 0.15$ (✱),$(y_{H_2})_o = 0.30$ (□), $(y_{H_2})_o = 0.40$ (○), (P_o = 1.0 bar; $y_{I_o} = 0.55$; T = 308 K; the number of experimental points was reduced for a better visualization). The solid line is the model fit by the integral method.

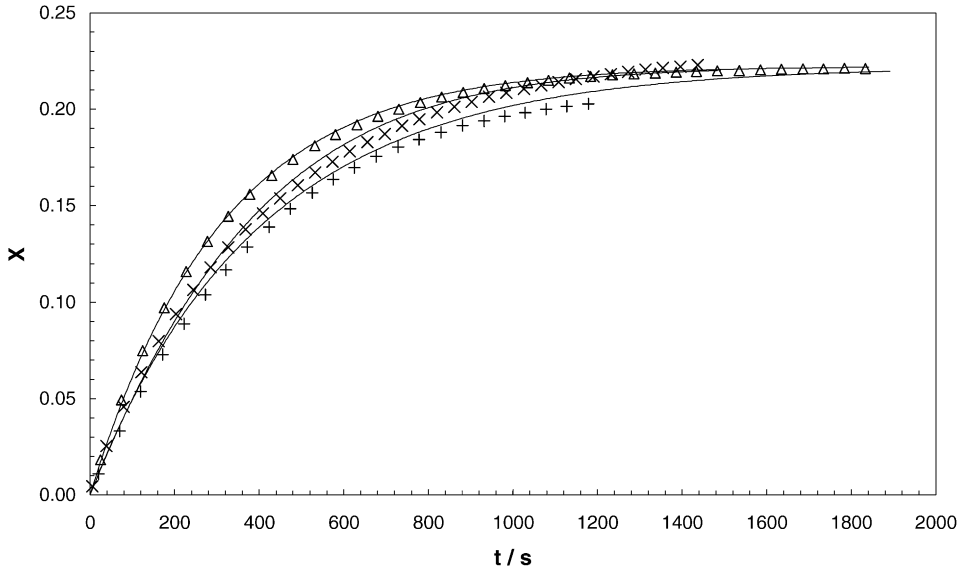

Fig. 5. Advancement of the reaction as a function of time for different initial total pressures: P_o = 0.50 bar (+), P_o = 1.0 bar (△), P_o = 3.5 bar (×) ($(y_{H_2})_o$: $(y_{C_3H_6})_o = 0.10 : 0.35$; T = 308 K; the number of experimental points was reduced for a better visualization). The solid line is the model fit by the integral method.

tion. Model 4 is based on the Houriti–Polany mechanism [9], with adsorption of the olefin in two sites. Model 5 was adapted for the present reaction and was first proposed by Borodzinski and Cybulki [35] for the selective hydrogenation of acetylene. Model 6 is also a LH equation that considers the bimolecular shock between the adsorbed propylene and the first hydrogen atom, followed by the addition of the second hydrogen atom. Finally, model 7 is the Rideal–Eley mechanism. However, the best model after using the MSC adopted is model 1, which is proposed in the present work.

For validation of both the proposed rate law and the kinetic parameters determined by the nonlinear regression, the integral method was used [28]. For that, Eq. (4) was integrated using the rate law shown in Eq. (8) and the kinetic parameters from Table 1. Assuming once again ideal gas behaviour, the hydrogen and propylene partial pressures in the rate equation were substituted from their dependence on the advancement of the reaction.

$$P_j = P_o[y_{j_o} - (1 - y_{I_o})X] \tag{10}$$

Figs. 4 and 5 show the plots of some experimental and theoretical curves. In all cases, integration of the mass balance describes quite reasonably the experimental advancement data. Although conversion of the limiting reactant j was always complete, the advancement curves tend to a maximum value which depends on the initial conditions.

$$X_{max} = \frac{y_{j_o}}{(1 - y_{I_o})} \tag{11}$$

For instance, in Fig. 4, the curves for $(y_{H_2})_o = 0.05$ or 0.40 tend both to X_{max} = 0.111, while for $(y_{H_2})_o = 0.15$ or 0.30, the limit value is 0.333. In Fig. 5, all the curves tend to the same X_{max} value (0.222).

5. Conclusions

In the present paper, the kinetics of propylene hydrogenation was studied under isothermal conditions using palladium nanosized clusters as catalyst. Because metal nanoclusters are not stable, as they quickly grow and/or fuse together into micrometric aggregates, surfactant-stabilised Pd nanoparticles were used. The technique used to immobilise the catalyst nanoparticles in a textile support, which involves dispersion in a THF solvent, does not affect the structure and dimensions of the catalyst aggregates, for which mass transport resistances are negligible. Besides, SEM/EDS analyses also showed that clusters do not lose their surfactant shell upon such treatment.

Although it was not possible to determine the active surface area of the supported catalyst before and after the hydrogenation reaction, it is reasonable to assume that it possibly remains unchanged, once reaction rates were quite reproducible.

The method of initial rates was adopted to establish the reaction mechanism. Although this approach does not exclude other reaction schemes, it was found that experimental rate data are coherent with a LH mechanism that involves competitive adsorption between reactants for the catalyst surface, with dissociative adsorption of hydrogen, and where surface reaction is the limiting step. The results agree with a Houriuti–Polanyi mechanism [9], but here it is involved one single site, not two, for olefin adsorption.

The corresponding LH rate equation represents very reasonably the experimental data of propylene hydrogenation, with the kinetic parameters being determined by nonlinear regression analysis.

For validation of both the proposed rate law and the kinetic parameters obtained, the integral method was used. Upon integration of the mass balance, one can conclude that the theoretical and experimental advancement curves agree very well for various sets of experiments.

The rate law of propylene hydrogenation herein determined is crucial for subsequent modelling of a polymeric catalytic membrane reactor, which contains the palladium nanoclusters in the polymeric matrix of the membrane. It is remarkable that the reaction rate determined showed good response when comparing the simulated versus experimental data obtained in the PCMR, and this will be the aim of a future publication.

Acknowledgements

Lúcia Brandão is grateful to the Portuguese Foundation for Science and Technology (FCT) for her Ph.D. grant (reference SFRH/BD/3383/2000). Financial support by FCT through the project POCTI/32452/EQU/2000 is also acknowledged.

References

[1] J.D. Aiken III, R.G. Finke, J. Mol. Catal. A: Chem. 145 (1999) 1–44.
[2] M.T. Reetz, W. Helbig, S.A. Quaiser, U. Stimming, N. Breuer, R. Vogel, Science 267 (1995) 367–369.
[3] A. Züttel, C. Nützenadel, G. Schmid, C. Emmenegger, P. Sudan, L. Schlapbach, Appl. Surf. Sci. 162–163 (2000) 571–575.
[4] M.T. Reetz, S.A. Quaiser, R. Breinbauer, B. Tesche, Angew. Chem. Int. Ed. Engl. 34 (23–24) (1995) 2728–2730.
[5] H. Gao, Y. Xu, S. Liao, R. Liu, J. Liu, D. Li, D. Yu, Y. Zhao, Y. Fan, J. Membr. Sci. 106 (1995) 213–219.
[6] J.F. Ciebien, R.E. Cohen, A. Duran, Supramol. Sci. 5 (1–2) (1998) 31–39.
[7] F. Zaera, G.A. Somorjai, J. Am. Chem. Soc. 106 (8) (1984) 2288–2293.
[8] H. Öfner, F. Zaera, J. Phys. Chem. B 101 (3) (1997) 396–408.
[9] I. Horiuti, M. Polanyi, Trans. Faraday Soc. 30 (1934) 1164–1172.
[10] S. Naito, M. Tanimoto, J. Catal. 102 (1986) 377–385.
[11] A.V. Zeigarnik, R.E. Valdés-Pérez, O.N. Temkin, Langmuir 14 (16) (1998) 4510–4516.
[12] R. Campostrini, G. Carturan, R.M. Baraka, J. Mol. Catal. 78 (1993) 169–179.
[13] G.B. Rogers, M.M. Lih, O.A. Hougen, AIChE J. 12 (2) (1966) 369–377.
[14] G. Cocco, R. Campostrini, M.A. Cabras, G. Carturan, J. Mol. Catal. 94 (1994) 299–310.
[15] W.E. Stewart, R.H. Shabaker, Y.T. Lu, Chem. Eng. Sci. 43 (8) (1988) 2257–2262.
[16] M.T. Reetz, W. Helbig, J. Mol. Catal. A: Chem. 116 (16) (1994) 7401–7402.
[17] M.T. Reetz, M. Winter, R. Breinbauer, T. Thurn-Albrecht, W. Vogel, Chem. Eur. J. 7 (5) (2001) 1084–1094.
[18] C. Sachs, A. Pundt, R. Kircheim, M. Winter, M.T. Reetz, D. Fritsch, Phys. Rev. B 64 (7) (2001) 5408–5417.
[19] T.P. Beebe, J.T. Yates Jr., J. Am. Chem. Soc. 108 (4) (1986) 663–671.
[20] R.J. Koestner, M.A. Van Hove, G.A. Somorjai, J. Phys. Chem. 87 (2) (1983) 203–213.
[21] L.R. Petzold, A.C. Hindmarsh, LSODA, Computing and Mathematics Research Division, Lawrence Livermore National Laboratory, 1997.
[22] J.B. Butt, Reaction Kinetics and Reactor Design, second ed., Marcel Dekker, Inc., New York, 1999.
[23] P.B. Weisz, Z. Physik. Chem., Neue Folge 11 (1957) 1.
[24] R.R. Hudgins, Chem. Eng. Sci. 23 (1) (1968) 93–94.
[25] S.D. Jackson, N.J. Casey, J. Chem. Soc. Faraday Trans. 91 (18) (1995) 3269–3274.
[26] F. Delannay, Characterization of Heterogeneous Catalysts, Marcel Dekker, New York and Basel, 1984.
[27] J. Villermaux, Génie de la Réaction Chimique – Conception et Fonctionnement des Réacteurs, second ed., Tec & Doc – Lavoisier, Paris, 1993.
[28] G.F. Froment, K.B. Bischoff, Chemical Reactor Analysis and Design, second ed., Wiley, New York, 1990.
[29] K.H. Yang, O.A. Hougen, Chem. Eng. Prog. 46 (3) (1950) 147–157.
[30] J.R.J. Rennard, R.J. Kokes, J. Phys. Chem. 70 (8) (1966) 2543–2549.
[31] K. Christmann, Mol. Phys. 66 (1) (1989) 1–50.
[32] E. Wicke, H. Brodowsky, Hydrogen in palladium and palladium alloys, in: J. Völkl (Ed.), Hydrogen in Metals II. Application-oriented Properties, Springer-Verlag, Berlin, 1978 (Chapter 3).
[33] H. Öfner, F. Zaera, J. Am. Chem. Soc. 140 (37) (2002) 10982–10983.
[34] M. Aitake, Math. Sci. 14 (1976) 5.
[35] A. Borodzinski, A. Cybulki, Appl. Catal. A 198 (2000) 51–66.